

Project RADARS

Rocket Altitude Determination and Response System

Tim Drake, Matthew Muetzel, Colin Cummins, Mary Otten¹

Department of Aerospace and Mechanical Engineering Saint Louis University, St. Louis, Missouri 63108

Project RADARS provides autonomous altitude control to solid motor rockets during ascent. The system utilizes an air braking mechanism to adjust drag, thereby controlling altitude. MATLAB and OpenRocket simulations predict flight trajectory and apogee, while Computational Fluid Dynamics (CFD) in ANSYS and OpenFOAM assess airbrake effectiveness. The team is currently in the manufacturing phase, integrating the avionics and airbrakes for 5 test flights, to iteratively refine the control algorithm. This paper outlines the design process, simulation methods, and flight test procedures, emphasizing the project's objective of achieving precise altitude control.

Nomenclature

δ	Airbrake Deflection Angle
ρ	Density
θ	Flight Path Angle
C_D	Total Coefficient of Drag
C_{DAB}	Drag Coefficient from Airbrakes
$Drag$	Total Drag
l_{AB}	Airbrake Length
num_{AB}	Number of Airbrakes
SM	Stability Margin
S_{ref}	Rocket Reference Area
S_{AB}	Airbrake Area
V	Velocity
w_{AB}	Airbrake Width

I. Introduction

Every year, collegiate rocketry teams participate in competitions to launch their rockets to a specified altitude with the winner being the team closest to the altitude requirement. Analysis of past competition found that teams often overachieve and fly beyond the threshold. This paper outlines a senior design project aimed to address this issue with a Rocket Altitude Determination and Response System (RADARS), designed to achieve an altitude of 5,000 \pm 50 ft.

Project RADARS focuses on integrating an airbrake control system into the rocket, enabling real-time deceleration during ascent, through increased drag due to airbrake deflection. The altitude control system will continuously compute the necessary drag to achieve the desired altitude and adjust the airbrakes accordingly throughout coast flight.

The control system and airbrake effectiveness will be tested through 5 flights. The first flight will not contain any airbrake deployment and provide a baseline rocket performance, required to reach an apogee above 5,600 feet. The 4 additional flights will further refine and test the air braking algorithm with the requirement to reach an apogee of 5,000 ft with 50 ft of margin on each end.

¹Undergraduate Student, Aerospace and Mechanical Engineering, and AIAA Student Member.

This paper discusses the analyses used to design and develop both the rocket and the control system, with the central ideas lying in the drag calculation and the principles of projectile motion. Explanations of these formulas and the work done with them can be found later in the report.

With future collegiate competitions in mind, particularly those involving Saint Louis University's Rocket Lab, Project RADARS serves as a proof-of-concept study for implementing dynamic altitude control systems. The project aims to develop an active dynamic altitude control system for future Saint Louis University Rocket Lab use.

II. Concepts of Operations

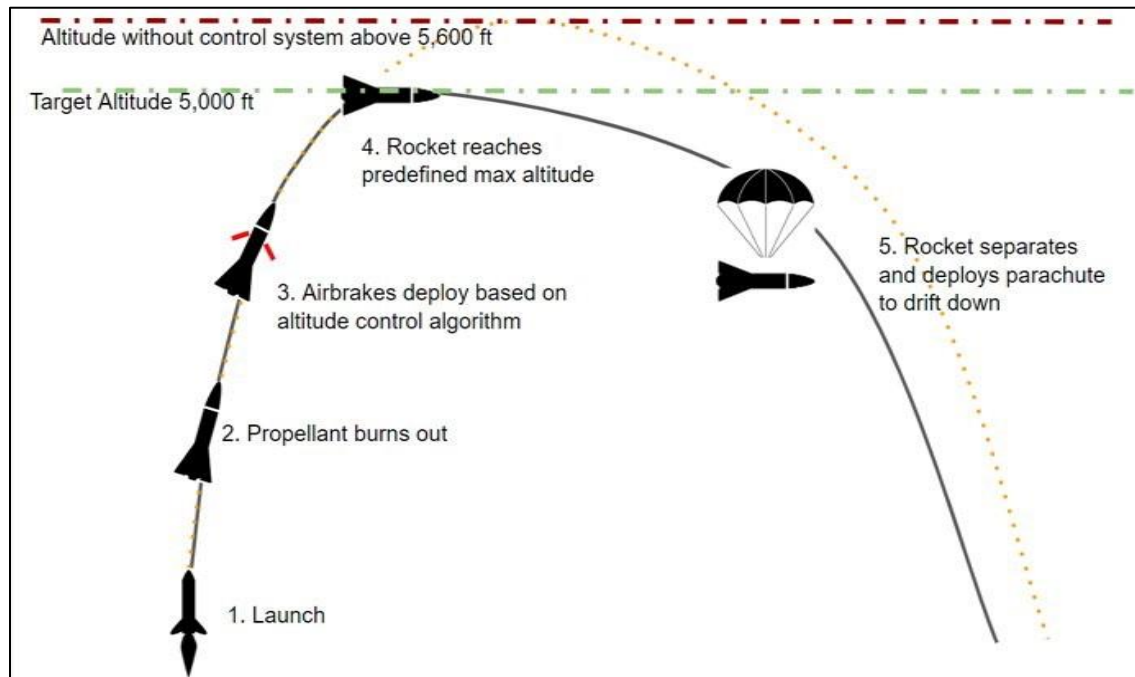


Figure 1: Mission Concept of Operations

Figure 1 above displays the concept of operations for Project RADAR broken down into 5 phases: Launch, Propellant Burnout, Airbrake Controlled Coast, Apogee, Descent/Touchdown and Recovery.

Phase 1, Launch, starts with the rocket mounted on the launch rod and prepared to launch. This phase includes turning on all the electronics with the use of screw switches then igniting the motor a safe distance away.

Phase 2, Powered Ascent, will last around 3.5 seconds propelling the rocket to an altitude of around 1,750 ft, with a vertical velocity around 670 ft/s at motor burn out. Momentum from this phase will carry the rocket to apogee in the coast phase.

Phase 3, Airbrake Controlled Coast, is the phase that will be the most active throughout the flight. This is the only phase where the airbrakes will actively deploy to reach the desired altitude of 5,000 ft. With the momentum from the Burn Phase the airbrakes will induce drag on the rocket decreasing the momentum to the target altitude of 5,000 ft given by the green line in Figure 1 above. This phase will last around 12-17 seconds with the variation depending on the magnitude the rocket is slowed by the airbrakes.

Phase 4, Apogee, is the maximum height the rocket will reach. In this phase the rocket will lose all vertical momentum and come to a complete vertical stop. Sensors on the rocket will detect this and ignite forward ejection charges separating the upper airframe from the coupler section and deploying a drogue parachute. The altitude control system will no longer be used, and the airbrakes are retracted just before apogee to prevent damage.

Phase 5, Recovery, includes the drogue descent, main descent, and touchdown of the rocket. The drogue descent starts as soon as the upper airframe separates from the coupler and the drogue parachute deploys. This descent will last around 45 seconds descending at a rate of 100 ft/s. Once the rocket descends to 500 ft the main deployment ejection charges ignite causing the coupler and booster section to separate. The main parachute will decelerate the rocket to 20 ft/s, carrying the rocket to touchdown in around 25 seconds. Finally, the rocket will touchdown and the team will follow the GPS transmitter to the rocket's location and complete the recovery.

III. Rocket Design and Construction

A. Design Drivers

Various design drivers were considered; however, the critical aspects were reliability, reusability, and accessibility. The team is looking for a reliable onboard system to continuously collect data throughout the flight and calculate the airbrake deployment angle needed to reach the target apogee. This challenged the team to develop a system that could rapidly respond to changes in a flight path and correct any unforeseen errors that occurred accurately. Second, both the entirety of the rocket and the altitude control system must be reusable, with the motor reload being the sole exception. Multiple test flights are necessary to refine the air braking algorithm. Thus, the rocket must be reusable as the data gathered from test flights will be specific to the rocket launched. This driver will save the team on cost and allow for usage in future Saint Louis University Rocket Propulsion Lab launches and competitions. Finally, the last significant design driver is accessibility. Project RADARS aims to use resources from Saint Louis University's Rocket Lab and Rocket Lab alums as mentors, making the team more cost-effective. This driver determined various trade study decisions, as explained in the following section.

B. Rocket Design

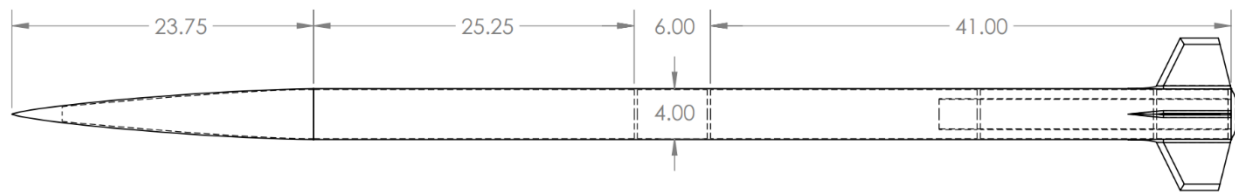


Figure 2: Rocket Component Design

Figure 2 displays the final rocket design with dimensions used within each section. The Haack Series nose cone was selected because it carried no cost as the team already had it in their possession and the performance was sufficient for the project.

The upper airframe will hold the main chute, shock cord, and black powder ejection components, and will be made of fiberglass to ensure radio frequency transparency. The length was chosen due to the required parachute volume.

The coupler is also made of fiberglass and will hold all the avionics and airbrakes. Its size was again chosen through consideration of the airbrake and avionic sled sizes. This section will house all the electronics and power required both for the rocket and the airbrakes, as well as the airbrakes themselves. The airbrake selection and design will be discussed later in the report.

The lower airframe consists of fins, bulkheads, motor mount, and centering rings. Four fins were selected as the team wanted to offset the fins from the four airbrakes. Additionally, the trapezoidal fin size was iteratively selected through various OpenRocket simulations comparing both the stability and apogee altitude. The low airframe length was again selected to ensure its volume could hold the motor mount and the main parachute, while the material is made of manufactured carbon fiber for its strength.

Lastly, in the motor section, the nozzle, O-rings, fuel grains, and Aerotech K700 motor are housed. Motor selection involved simulating various options and assessing criteria such as cost, performance, reliability, and availability. Ultimately landing on the Aerotech K700 motor.

C. Manufacturing Process

Various parts of the rocket were manufactured in the lab, with some parts being purchased from outside suppliers. Multiple manufacturing methods were used across the entire rocket with the use of 3D printers, carbon fiber winder, water jet, lathe, and mill.

The lower air frame and motor mount were constructed in the lab using an X-Winder. Circular inserts were cut out of 2 in. foam insulation using a water jet. Five layers of carbon tow was wound around the foam to the required diameter. The tubes were cut down to the required length and sanded for smoothness.



Figure 3: X-Winder Lower Airframe Tube Winding



Figure 4: Tail Cone Manufacturing

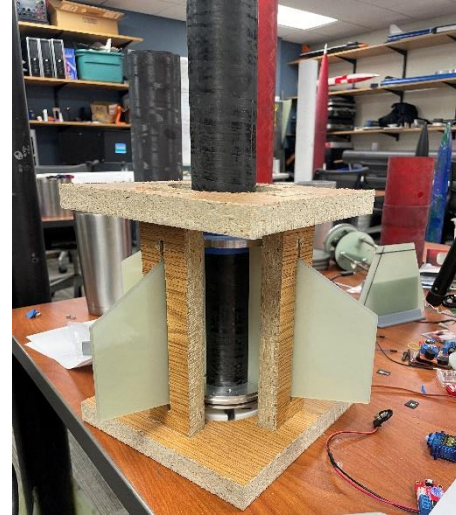


Figure 5: Fin Mounting

The upper airframe and coupler were purchased from an outside supplier as stock fiber glass tubes then cut down using a miter saw to satisfy each part's project length requirements. The fins were first purchased from an outside supplier as an 1/8" fiberglass sheet and then cut down to the correct shape using a water jet.

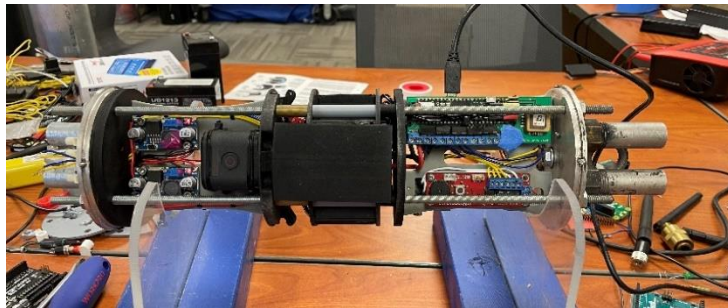


Figure 6: Avionics Bay Construction

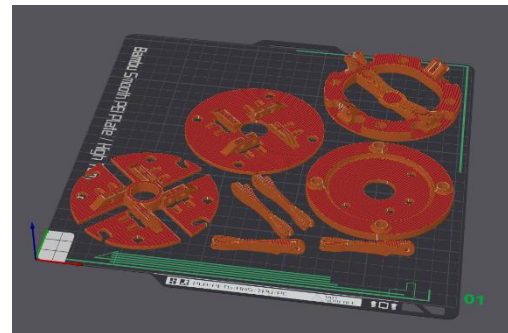


Figure 7: 3D Printed Parts

Finally, the aluminum centering rings, tail cone, and magnesium bulkheads were machined by the team using a combination of a lathe and mill. Once these parts were constructed, the motor mount, centering rings, and fins were epoxied together inside a jig ensuring the fins were perpendicular. Four slits were cut in the bottom of the lower airframe to slide the fin can into position. Holes for vents, shear pins, and screw switches were drilled into the airframe once the avionics bay was fully configured.

The avionics sled was primarily manufactured using the rocket labs Bambu X1 Carbon 3D printer. This allowed the team to quickly modify the design and placement of mounts, computers, and other components. Test pieces were printed in PLA and ABS plastic, and the final load bearing pieces were printed in solid infill PLA-CF filament.

D. Mass Properties

The mass of the rocket is very important in determining the expected apogee and stability. With this in consideration the team created a mass properties table to ensure the predicted mass was reasonable and the following preflight design analyses were reasonable. The final rocket mass was expected to weigh a total of 16.77 lbs. However, the team added a tolerance of 15% for each part. Thus, allowing a total of 19.285 lbs the rocket to reach the minimum non-airbrake flight apogee of 5,600 feet. With construction complete it was found to be around 17.4 lbs, which while larger than expected the weight is still within the added tolerance.

IV. Performance Analysis

A. Altitude Performance

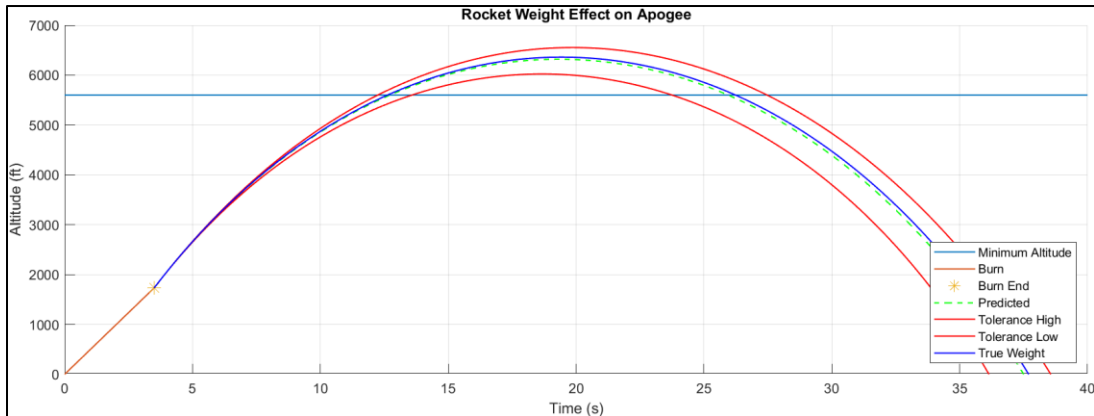


Figure 8: Altitude Plot for no Airbrake Deflection

As can be seen in Figure 8, the designed rocket is expected to reach an altitude of around 6,600 feet for both the predicted and true mass. This altitude is 1,000 feet above the minimum altitude of 5,600 feet for flight without airbrakes. It is important that this tolerance is given as the model used to predict drag assumes perfect transitions across the body tubes and the fin connections. In true practice this will not take place so the team designed a rocket well above the minimum requirements. Both the high and low tolerances are well above the minimum altitude.

B. Stability Performance

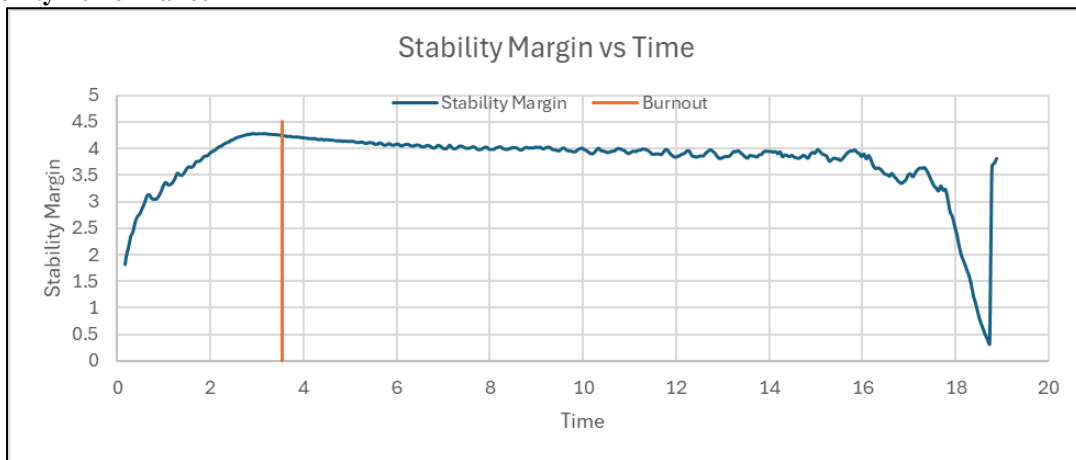


Figure 9: Stability vs. Time Throughout Flight

As shown by Figure 9, the designed rocket is very stable, with a stability margin, SM , of 1.7 at the rail exit and hovering around 4.0 for most of the flight. This well exceeds the standard practice of a stability margin above 1.0 throughout the flight. However, this extra stability is necessary as airbrake deployment will move the center of pressure forward along the rocket, decreasing the SM . The team has attempted to account for the airbrake's effect on stability

in OpenRocket by adding thick fins, as seen in *Figure 5* below. However, OpenRocket cannot accurately predict flow around thick fins, and was disregarded.

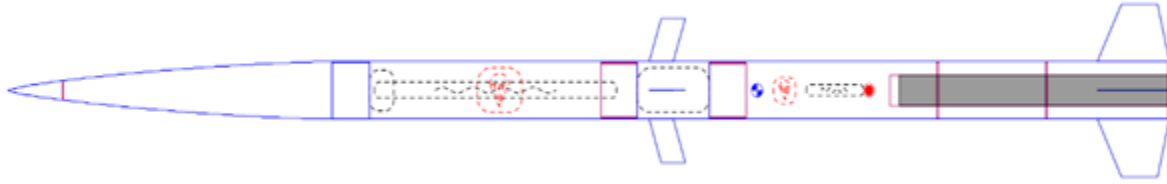


Figure 10: OpenRocket Stability Simulation Using "Thick" Fins

While there is no concrete analysis on the stability the team is confident that the airbrake location will not move the center of pressure above the center of gravity, as it would have to move over 12 inches along the rocket body. Additionally, with a 300% tolerance stability should not be an issue.

V. Airbrake Analysis

A. Altitude Control Trade Studies

The altitude control system trade studies involved two parts: selecting the type of altitude control system and further analyzing the chosen air braking system's design. The team selected modular downward facing flaps, seen in *Figure 11* that can angularly deflect to any angle 0° - 90° for their high controllability and reusability aligning with project success goals.

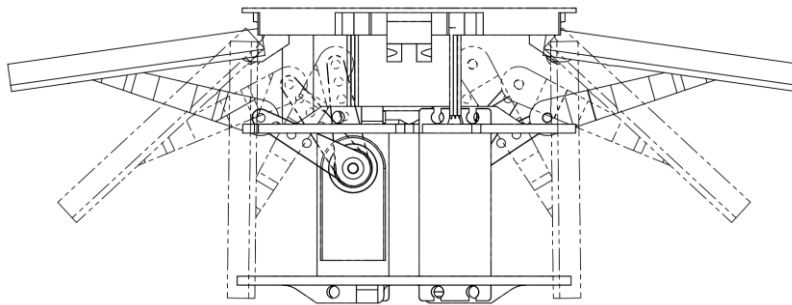


Figure 11: Side View of Modular Downward Facing Flaps

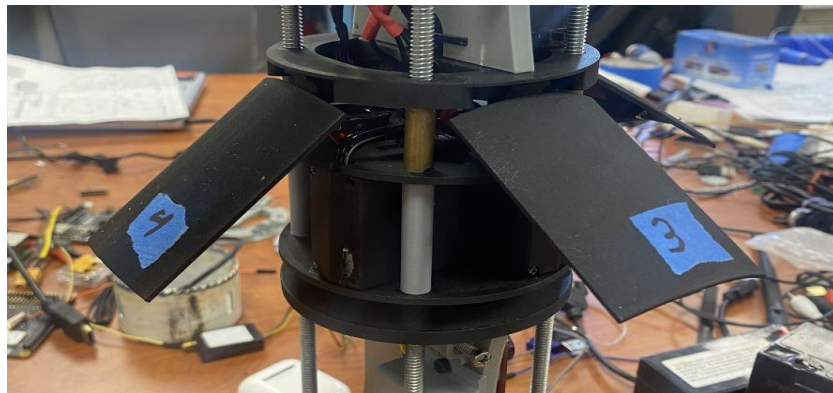


Figure 12: Carbon 3D Print Airbrakes

The airbrakes consist of four carbon fiber 3D printed 2-in by 3-in airbrakes each 90° apart as seen in *Figure 12* above. The rocket circumference being around 12.5-in led to the 2-in width, as anything larger would have decreased this distance between the brakes leading to structural questions, while anything smaller would have led to a respective increase in length and a larger moment on the mechanism. With the airbrake width determined the team determined a 3-inch span would provide sufficient drag and control for this mission scope.

The range of locations for the airbrakes was limited by aerodynamic and stability considerations. If the brakes were positioned too low, the airflow would not be able to settle in time for when the fins provide their stability, while if too high air brakes deflection result in an unstable rocket. With these considerations, the airbrakes were placed 45-

in from the rocket base. This selection was largely qualitative when determining if there would be enough room in the lower airframe for the parachute, shock cord, and motor. However, various CFD simulations were performed to ensure the location maintained a positive stability margin and the flow decreased turbulence near the fins. An additional way the team will ensure stability near the fins is offsetting the brakes by 45° from the fins to from the fins to reduce the downwash effect created by the turbulent airflow.

B. System Design

Airbrakes are commonly used in modern rockets such as SpaceX's grid fins. The fins allow greater yaw and roll stability when deflected using hydraulic actuators. While hydraulic actuators are ideal for deflecting high forces, they are too large to fit in a 4-inch body tube. Other designs for model rocket airbrakes include stepper motors attached to a threaded rod which deflects all airbrakes at once. While this is the simplest design, our team wanted to ensure our airbrakes will individually actuate, allowing for future teams to control the stability of the rocket. This led to selecting servos using moment arms to hinge the airbrakes into position. The four large servos can fit in the 4-inch body tube with a custom back plate that contours to the shell of the coupler.

The basic configuration of the avionics sled is like a sandwich. The sled consists of three sections separated by plates that are the inside diameter of the coupler tube; these are known as bulkheads. These bulkheads are aligned by 4 1/4-20 threaded rods to prevent them from rotating. Each bulkhead is spaced accordingly using cylinders around the threaded rod and vertical mounts. The airbrakes and aft coupler bulkhead must be removed to allow the avionics sled to slide into the coupler tube. Finally, the aft coupler bulkhead is reattached and tightened to keep the sled in place and the airbrakes are mounted.

Servos draw a lot of current while under load. If the servos are powered through the flight computer, it may cause the computer to heat up. To prevent this, the servos are directly powered by the same 7.4V LiPo as the flight computer and two DC-DC voltage regulators were added to step the voltage down to the 6V operating voltage of the servos.

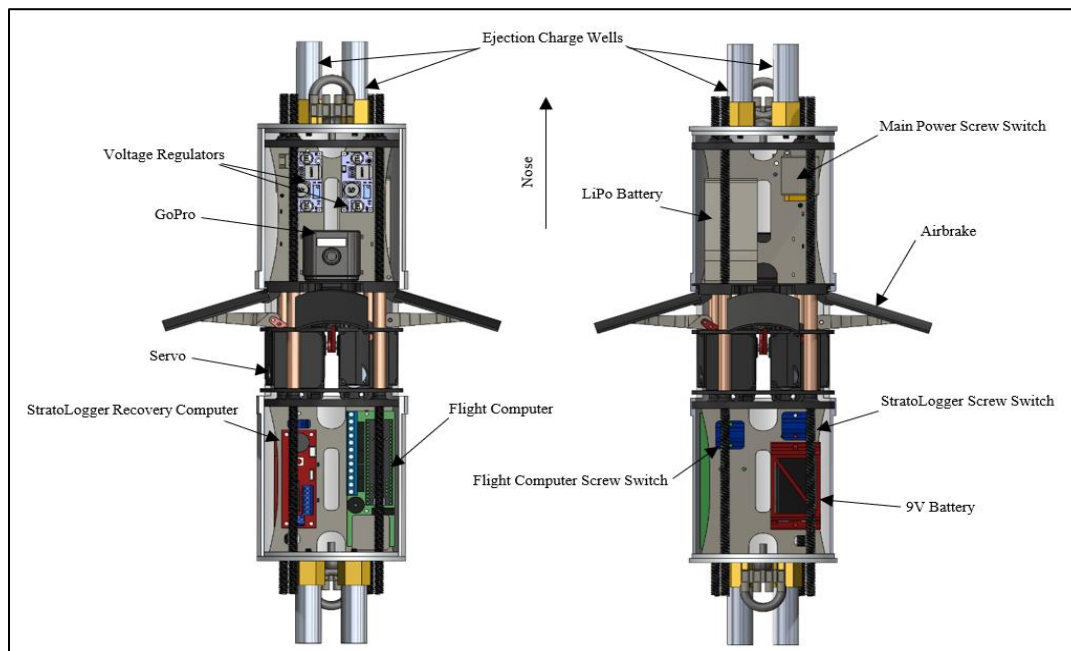


Figure 13: Avionics Sled Cross-Section

Figure 13 illustrates the front and back configuration of the avionics coupler. The aft section consists of the flight computer, StratoLogger, 9V battery, and screw switches for each computer. Screw switches are used to turn on all avionics while the rocket is sitting on the launch pad. A small hole is cut in the airframe to allow a screwdriver to turn a screw into a nut which completes the switches circuit. The forward section of the sled houses the two DC-DC voltage regulators, 7.4V LiPo battery, main power screw switch, and a GoPro. A similar design is used for the main power screw switch in the forward section, where this completes the positive connection to the battery allowing power to all components. The GoPro will record the inside of the sled facing down to confirm the airbrakes deploy correctly throughout the flight. Two black powder wells are attached to the forward and aft bulkheads. These are used to separate the sections of the rocket and deploy parachutes after apogee. One well on each bulkhead is wired to the StratoLogger

and the other to the flight computer. If the StratoLogger fails in flight, the flight computer acts as a redundant recovery computer and the well connected will ignite. In the case where both computers are working, the flight computer is set at a slightly lower altitude to ignite its charges to prevent both charges igniting at the same time inside the rocket which can damage the parachutes.

C. Aerodynamic Analysis

One of the primary drivers of the airbrake performance is the drag they create. This drag will create a force on the rocket and decrease the rocket's acceleration. Thus, the team must understand the aerodynamic forces acting on the rocket to develop the aerobraking algorithm properly.

The team initially planned to perform aerodynamic studies using one of Saint Louis University's low-speed or high-speed wind tunnels. From Reynolds Number matching, it was found that using the sub-sonic wind tunnel to test the behavior of the rocket was impossible due to the max speed of wind tunnel. The supersonic wind tunnel's balance was not operational, so no viable data could be gathered. Thus, the team performed a complete aerodynamic analysis using Computational Fluid Dynamics (CFD). This decision adds a lot of risk as the results will primarily be from simulations rather than experimental tests. Thus, the team hopes to mitigate this risk with added flight tests built into the schedule and budget.

a. ANSYS CFD Analysis

The team started out primarily using SolidWorks to model the rocket and ANSYS simulate the flow surrounding the rocket. A grid independence study was tried to determine the optimal enclosure and mesh size throughout the simulation. However, being restricted to the student version of ANSYS the team failed to produce a mesh that they felt accurately portrayed the flow surrounding the rocket. Thus, the team made the switch to OpenFoam in hopes that an open software would provide stronger results, as it would not restrict the students in the same way ANSYS does. Additionally, OpenFoam was found to take much less time than ANSYS simulations.

b. OpenFoam Analysis

With OpenFoam the team again used a mesh convergence study whose table can be seen below for a 60° airbrake deflection. The mesh independence study focused on selecting a mesh grid allowing for accurate analysis while not overdoing the accuracy. The difference between the 4.7 million cell mesh and the 5.5 million cell mesh was found to only carry around a 5% error, which is sufficient for the purposes of this study. Thus, the 4.7 million cell mesh will be used to calculate other Coefficient of drag values at the various airbrake deflection angles.

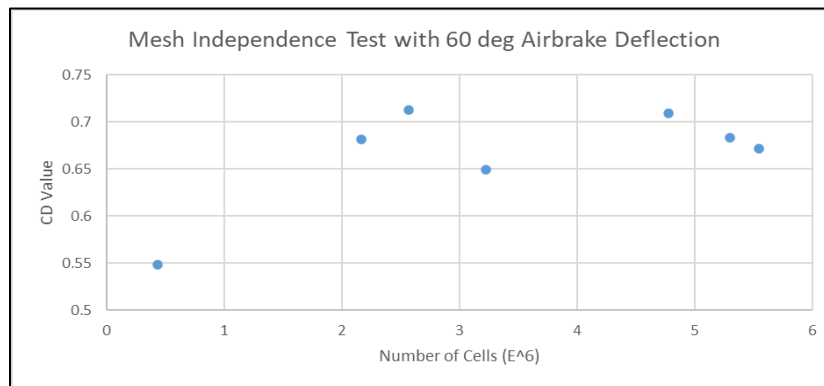


Figure 14: Mesh Independence Test

Steady state simulations were run using rhoSimpleFoam, a compressible flow solver included in OpenFOAM. To predict how much drag will be produced, multiple 3D models were created and simulated for every 5° of airbrake deflection. Utilizing OpenFOAM's open-source software, a script was written to simulate all 20 models and tabulate the CD values collected after 500 simulated time steps. The simulated time was selected to ensure the simulation fully converged. Figure 15 shows the convergence of the coefficients simulated on a model with 80° airbrake deflection after 500 simulated time steps:

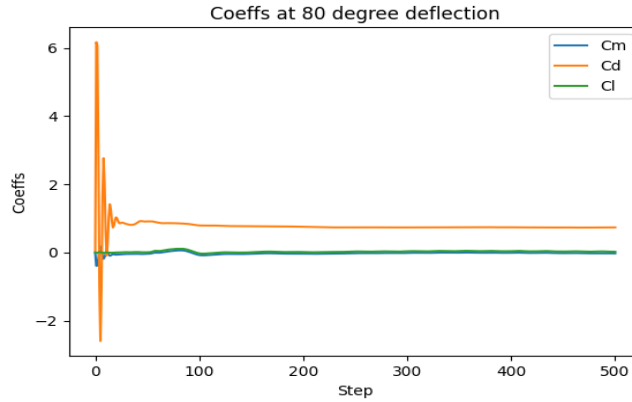


Figure 15: Simulated Coefficients for 80° Deflection

Each model was simulated at 671ft/s, the max velocity of the rocket. Since C_D is a non-dimensional number, the velocity should not affect the outcome of C_D . The team used Paraview to post process the simulations. Figure 16 visualizes the velocity gradient across the rocket with a 60° deflection:

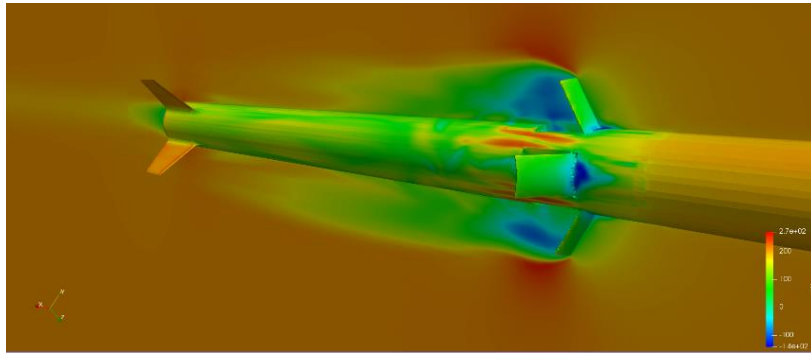


Figure 16: Paraview Post-Processing of 60° Model

D. Altitude Control Algorithm

The process of creating an altitude control algorithm began with identifying the data needed for the algorithm and identifying the capabilities of Colonel Bryan Sparkman's flight computer. The computer has a sensor package of GNSS, accelerometers, gyroscope, magnetometer, barometer, and LoRa radio and can capture approximately 50,000 samples per second.

Initially, it was thought that GNSS coordinates should be used during the flight to determine the rocket's location, acceleration, and drag to calculate a predicted apogee. However, after discussing with Sparkman, GNSS coordinates drop in accuracy as the speed of the rocket increases, more specifically it drops out after 5 G's, which is not sufficient for a predicted 11 G max acceleration before burnout. GNSS does become more stable and accurate later during flight and will be needed during the rocket's descent. The barometric pressure sensor is most accurate at lower speeds of the computer's systems since noise influences the sensor. As an alternative, the accelerometer provides the most accurate data than any other avionics sensor. The accelerometer will be used to calculate drag on the rocket and predict drag along the flight, and how much would we need to increase or decrease our drag to hit the peak altitude.

To do this, we first had to model a theoretical algorithm on what data our model would be intaking and what the outcome would be, and then adding the equations later.

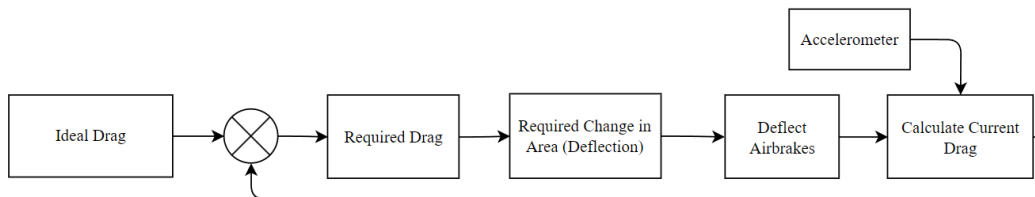


Figure 17: Altitude Control Diagram

Figure 17 models the algorithm as a closed loop system. Usually control loops have an error to check if the calculated value is accurate to the expected. In the case of servos, potentiometers are used to compare the input angle to the actual servo angle and correct accordingly. The servos used in the mechanism do not contain potentiometers, so the error used is the expected drag compared to the current acceleration.

We initially concluded that drag is not a linear calculation, which means apogee cannot be calculated at any point in flight. However, the ideal C_D value for a 5,000 ft apogee can be iteratively solved using the velocity and altitude at burnout. From this C_D value, a simulation of the drag produced throughout the ideal flight is tabulated. Using this method results in the airbrakes not immediately deflecting at burnout. While this is not ideal, the delay allows the rocket to slow down enough that the airbrakes are not at risk of becoming damaged. Once the ideal drag values are calculated, the current drag calculated from the accelerometer is used to calculate the required drag to slow the rocket to the ideal curve:

$$D_{current} = -\frac{a_{sensor} * g}{W \sin \theta} - T + W$$

$$\Delta D_{req} = D_{Ideal} - D_{current}$$

Using the current velocity (V_C) and area (S_C), the required $C_{D_{req}}$ is calculated, where C_{D_0} is the current C_D :

$$C_{D_{req}} = C_{D_0} + \frac{2\Delta D_{req}}{\rho V_C^2 S_C}$$

The new area and airbrake deflection angle are finally calculated:

$$\Delta S = \frac{2\Delta D_{req}}{\rho V_C^2 C_{D_{req}}}$$

$$\delta_{new} = \delta_0 + \sin^{-1} \left[\frac{\Delta S}{num_{AB} * w_{AB} * l_{AB}} \right]$$

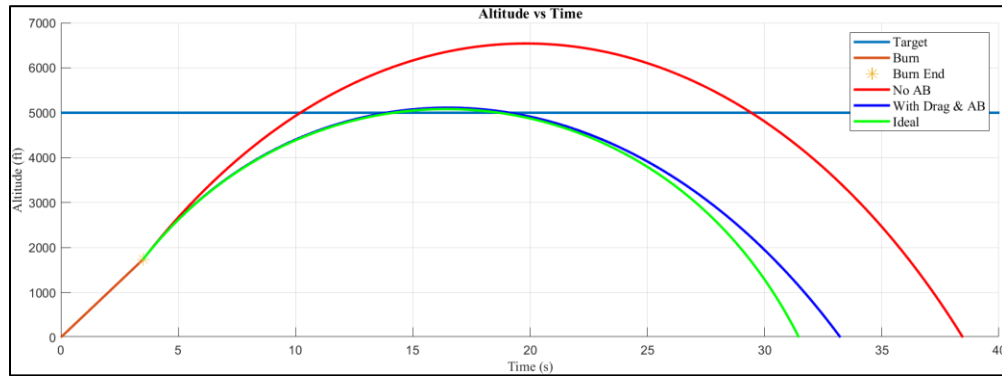


Figure 18: Altitude vs. Time of Rocket Flight

Figure 18 plots the simulated flights using basic projectile motion equations accounting for drag. While this algorithm works in MATLAB, the team now must convert the code to C and fully integrate the algorithm with Col. Sparkman's flight computer and code.

VI. Conclusion

With the completion of the design and manufacturing stage Project RADAR aims to prove their claims and fine tune the algorithm with true flight data. 5 launches are planned for this purpose with the first being on March 9th, 2024. Through each launch the team hopes to further refine the algorithm and address and design flaws. Ultimately leading to RADARS's success in reaching its designated altitude. The project's success hopes to aid future collegiate rocketry teams, particularly Saint Louis University Rocket Lab, to reach specified altitudes in rocketry competitions.